


MiR-203a-3p Inhibits Pancreatic Cancer Cell Proliferation, EMT, and Apoptosis by Regulating SLUG

Technology in Cancer Research & Treatment
Volume 19: 1-12
© The Author(s) 2020
Article reuse guidelines:
sagepub.com/journals-permissions
DOI: 10.1177/1533033819898729
journals.sagepub.com/home/tct


Ning An, BD¹ and Bo Zheng, BD¹ 

Abstract

Objective: The aim of the present research is to study the roles of miR-203a-3p on cell proliferation, migration, invasion, and epithelial–mesenchymal transition in pancreatic cancer. **Methods:** Transcription profiles were acquired from Gene Expression Omnibus database, which was used to screen out the differentially expressed microRNAs and messenger RNAs in pancreatic cancer. Pancreatic cancer tissues were used to verify the bioinformatics results by quantitative real-time polymerase chain reaction. The relationship between miR-203a-3p and SLUG was examined by TargetScan software, dual-luciferase reporter assay, and RNA immunoprecipitation. The Cell Counting Kit-8, wound healing, and transwell assays were conducted to investigate the proliferation, migration, and invasion capability of pancreatic cancer cells, respectively. The expression of epithelial–mesenchymal transition–related proteins was determined by the Western blot assay. Xenograft assay was performed to verify findings from *in vitro* assays. **Results:** Bioinformatic analysis found that a total of 113 microRNAs and 1749 messenger RNAs expressed differentially in pancreatic cancer tissues. Among these microRNAs, the expression of miR-203a-3p was significantly decreased in both pancreatic cancer tissues and cells. On the other hand, the SLUG expression was remarkably upregulated in pancreatic cancer tissues and cells in comparison with normal tissues and cells. Moreover, TargetScan software, dual-luciferase reporter assay, and RNA immunoprecipitation revealed that SLUG was a target of miR-203a-3p. The upregulation of miR-203a-3p expression inhibited the proliferation, migration, and invasion ability of pancreatic cancer cells by suppressing the epithelial–mesenchymal transition process via sponging SLUG. **Conclusion:** These findings indicate that downregulation of miR-203a-3p in pancreatic cancer cells leads to high expression of SLUG, which promotes epithelial–mesenchymal transition process and induces cancer progression.

Keywords

pancreatic cancer, miR-203a-3p, SLUG, EMT, miRNAs

Abbreviations

CCK-8, Cell Counting Kit-8; cDNA, complementary DNA; EMT, epithelial–mesenchymal transition; FBS, fetal bovine serum; GAPDH, glyceraldehyde 3-phosphate dehydrogenase; miRNA, microRNA; mRNA, messenger RNA; NC, negative control; PC, pancreatic cancer; qRT–PCT, quantitative real-time–polymerase chain reaction; si-SLUG, siRNA against for SLUG; 3′-UTR, 3′-untranslated region; ZEB1, zinc finger e-box binding homeobox 1

Received: November 22, 2018; Revised: July 31, 2019; Accepted: November 08, 2019.

Introduction

The fourth most common cause of cancer-related mortality in the United States is pancreatic cancer (PC), and it is estimated that PC could have the second highest mortality rate among cancers by 2030.¹ Pancreatic cancer has a poor prognosis as PC progresses rapidly and metastasizes even in the early stages.² On the other hand, current systemic therapy for PC is limited and with a modest efficacy.³ Moreover, patients with PC

¹ Department of Hepatological Surgery, Sichuan Academy of Medical Sciences & Sichuan Provincial People's Hospital, Chengdu, China

Corresponding Author:

Bo Zheng, Department of Hepatobiliary Surgery, Sichuan Academy of Medical Sciences & Sichuan Provincial People's Hospital, No. 32 West Second Section First Ring Road, Chengdu 610072, Sichuan, China.
Email: 2364912746@qq.com



Creative Commons Non Commercial CC BY-NC: This article is distributed under the terms of the Creative Commons Attribution-NonCommercial 4.0 License (<https://creativecommons.org/licenses/by-nc/4.0/>) which permits non-commercial use, reproduction and distribution of the work without further permission provided the original work is attributed as specified on the SAGE and Open Access pages (<https://us.sagepub.com/en-us/nam/open-access-at-sage>).

frequently obtain multidrug resistance.² The majority of patients who present with the localized disease eventually develop metastasis. Therefore, it is essential to develop novel systemic therapies to improve therapeutic outcomes.

MicroRNAs (miRNAs) are small noncoding RNA molecules composed of approximately 19 to 25 nucleotides.⁴ MicroRNAs are mainly related to the posttranscriptional regulation, which bind to the 3'-untranslated region (3'-UTR) of target messenger RNAs (mRNAs), resulting in either translation repression or mRNA degradation.⁵ Many recent researches have focused on the biological function of miRNAs and revealed that miRNAs involve many fundamental biological processes, including cell proliferation, differentiation, migration, survival, and apoptosis.⁶ miR-203 is the miRNA found on the chromosome 14q32.33 and plays important roles in human tumorigenesis. In renal cell carcinoma, for instance, miR-203a targets glycogen synthase kinase-3 β , promoting cell proliferation and migration.⁷ In many cancers, it is found that the expression of miR-203 is downregulated, for example, the prostate cancer, hepatocellular carcinoma, and esophageal squamous lung carcinoma, and previous studies have shown that miR-203 exhibits potent antiproliferative function.^{8,9} However, the role of miR-203a-3p and its molecular regulation mechanism in PC is less reported and requires further investigation.

SLUG, as known as SNAIL2, is a transcription factor that regulates epithelial–mesenchymal transition (EMT) process in cancer progression.¹⁰ SLUG can facilitate cancer cell metastasis and invasion by suppressing the epithelial phenotype and initiating EMT via binding to E-box DNA sequences found within the proximal promoter region of the E-cadherin gene.^{11,12} In addition, altered SLUG expression has been found in several cancers. For example, it has been demonstrated that SLUG is consistently upregulated in breast tumors.¹³ Upregulation of SLUG promotes EMT and thus metastasis of breast cancers.¹⁴ Related researches have also shown that the expression of SLUG is related to poor prognosis in PC patients.¹⁵

Epithelial–mesenchymal transition refers to the conversion of epithelial cells to mesenchymal cells by losing cell–cell junction and apical-basal polarity while gaining a high motility and invasive phenotype.¹⁶ Epithelial–mesenchymal transition plays an important part information of embryo and development of organs, as well as tissue fibrosis and wound healing.¹⁷ With EMT, cells obtain cancer stem cell-like features and can invade across basement membranes and stromal tissues.¹⁸ Therefore, EMT contributes to the progression of cancer by promoting cell migration and invasion.¹⁹

In our present research, we studied the possible relationship between miR-203a-3p and the invasion and migration of PC cells. Our findings are expected to offer a theoretical basis for the research and development of new targeted therapies for PC.

Materials and Methods

Transcriptomics Analysis

GSE71533 and GSE16515 were obtained from the Gene Expression Omnibus database (<http://www.ncbi.nlm.nih.gov/>

<http://www.ncbi.nlm.nih.gov/>). Total RNA was extracted from formalin-fixed and paraffin-embedded samples obtained from PC patients. By GSE71533, the miRNA expression profiling is done on tumor and normal adjacent tissues using miRCURY LNA™ microRNA Array 7th arrays. Through GSE16515, microarrays were conducted to identify difference in mRNAs expression between normal tissues and PC tissues. The gene profiles of PC and normal samples were analyzed by R software. Specific genes were screened out by following the criterion of $|\text{Log}_2(\text{fold change})| > 2$ and $P < .05$.

Cell Culture

The PANC-1, AsPC-1, Capan-1, and SW 1990 (human PC cell lines) as well as HPC-Y5 (normal pancreatic epithelial cell line) were purchased from the American Type Culture Collection (ATCC, Manassas, Virginia). Dulbecco's modified Eagle's medium supplemented with 2-mM L-glutamine, 10% fetal bovine serum (FBS), and 100U/mL penicillin/streptomycin was used to culture cells. Cells were cultured at 37°C with a supply of 5% CO₂.

Cell Transfection

Pancreatic cancer cells for *in vitro* assays were transfected with negative control (NC), siRNA against for SLUG (si-SLUG), miR-203a-3p mimic, miR-203a-3p inhibitor, or si-SLUG and miR-203a-3p inhibitor (si-SLUG + miR inhibitor). All those small molecules in this experiment were obtained from GenePharma (Shanghai, China). Lipofectamine 3000 purchased from Solarbio (Beijing, China) was used to perform transfection. Forty-eight hours post-transfection, cells were harvested for transfection efficiency test.

Quantitative Real-Time Polymerase Chain Reaction

PureLink RNA Mini Kit (Invitrogen, Carlsbad, California) was used to extract RNAs. The PrimeScrip RT reagent kit (Takara, Shiga, Japan) was used to synthesize first-strand complementary DNA (cDNA). The reaction system included 0.2- μ L sense and antisense primers, 2- μ L cDNA, and iQ SYBR Green supermix (Bio-Rad, California, USA). The parameters of PCR were as follows: 50°C for 2 minutes, 95°C for 2 minutes, and 40 cycles of 95°C for 15 seconds and finally 60°C for 1 minute. U6 and glyceraldehyde 3-phosphate dehydrogenase (GAPDH) was chosen as the endogenous control for miR-203a-3p and SLUG, respectively. Gene expression was quantified by the $2^{-\Delta\Delta C_t}$ method.

Cell Counting Kit-8 Assay

Cell Counting Kit-8 (CCK-8; Dojindo Co., Ltd, Kumamoto, Japan) monitored the proliferation ability of cells. After transfection for 12 to 24 hours, suspensions of transfected cells were put into 96-well plates (100 μ L/well; 4000 cells/well) and incubated at 37°C under the condition of 5% CO₂. During 0, 12, 24, and 48 hours of incubation, CCK-8 solution (10 μ L/well) was added to each well and cells were incubated for 1 to 4 hours.

Multiskan FC microplate reader (Thermo Fisher Scientific, Waltham, Massachusetts, USA) was used to detect the optical density value of cell suspension at 450 nm wavelength. The experiment was performed 3 times.

Wound Healing Assay

Wound healing assay was applied to detect the migration ability of PC cells. First, cells from each group were cultured in 6-well plates. The monolayer cells were then scraped by a 200- μ L pipette tip to create 2 linear regions without cells and cultured in serum-free medium. ImagePro 6.0 (Media Cybernetic, Rockville, Maryland) was applied to capture and measure the scratch distance between the linear regions at different time points. The experiment was performed 3 times.

Transwell Assay

Transwell assay was performed for cell invasion test. Firstly, cells (5×10^4 cells; 200 μ L) were put into the upper chamber of transwell chambers precoated with Matrigel (BD Biosciences, San Jose, California). Dulbecco's modified Eagle's medium and 10% FBS were added to the lower chamber. Then, the Transwell chambers were placed in an incubator for 24 hours at 37°C, 5% CO₂. After incubation, cells were removed from the upper chamber and chamber membrane was washed with phosphate-buffered saline and soaked in 95% ethanol for 10 minutes. The crystal violet (0.1%) was used to stain the membrane for 10 minutes. The stained cells were washed with flowing water 3 times following air drying, counted under an inverted optical microscope (Nikon, Tokyo, Japan) and captured for the representative photographs. All the experiments were performed thrice.

Western Blot

First, PC cells or tissues were solubilized in cold lysis buffer and the extracted protein was detected by a BCA assay kit for protein concentration (Takara, Shiga, Japan). Then, the proteins were segregated through 10% sodium dodecyl sulphate-polyacrylamide gel electrophoresis (Bio-Rad, Hercules, California) and then placed into polyvinylidene fluoride membranes (Invitrogen) following the protocol. A 5% of nonfat milk was applied to seal the membrane for 1 hour and then the membrane was incubated with anti-E-Cadherin antibody (#ab15148, 1:500; Abcam, Cambridge, Massachusetts), anti-Twist antibody (#ab50581, 0.5 μ g/mL; Abcam), anti-N-Cadherin antibody (#ab18203, 1 μ g/mL; Abcam), anti-SLUG antibody (#ab106077, 1 μ g/mL; Abcam), and anti-GAPDH antibody (#ab9485, 1:2500; Abcam). The incubation was performed at 4°C for 1 night. Thereafter, membranes were incubated with the secondary antibody goat anti-rabbit IgG H&L (horseradish peroxidase) (#ab6721, 1:5000; Abcam) for 1 hour at 37°C. The immunoreactive proteins were observed through an enhanced chemiluminescent detection system (Thermo Fisher Scientific, Waltham, Massachusetts) and photographed

under a microscope (Bio-Rad). Glyceraldehyde 3-phosphate dehydrogenase was considered a reference protein. All the trials mentioned above were performed 3 times.

Dual-Luciferase Reporter Gene Assay

The HEK293 cells were grown in a 96-well plate at the density of 2.0×10^4 cells per well. Then, Lipofectamine 3000 (Invitrogen) was used to co-transfect HEK293 cells with 150 ng of pmir-GLO-SLUG-Wt or pmir-GLO-SLUG-Mut (Sangon Biotech, Shanghai, China) and 2 ng of pRL-TK (Promega, Madison, Wisconsin) with a miR-203a-3p mimic or miR-NC. After transfection for 48 hours, the relative activity of luciferase was calculated by normalizing firefly luciferase to renilla luciferase. Each experiment was duplicated 3 times.

RNA Immunoprecipitation

Magna RNA immunoprecipitation (RIP) kit purchased from Millipore (Bedford, Massachusetts) was used for RIP experiments according to the manufacturer's instruction.²⁰ Pancreatic cancer cells at approximately 80% confluence were collected and lysed in RIP lysis buffer, which contained RNase inhibitors and protease inhibitors (Roche, Basel, Switzerland). The cell lysates were incubated in RIP buffer containing magnetic beads with the conjugation of human anti-Ago2 antibody (Millipore) or IgG (NC). In addition, 10- μ L RIP mixture was used as input. Proteinase K treatment was used to release affiliated RNA. RNeasy MinElute Cleanup Kit (Qiagen, Düsseldorf, Germany) was used to extract immunoprecipitated RNA. The RNA was used for quantitative real-time polymerase chain reaction (qRT-PCR) analysis of miR-203a-3p and SLUG.

Xenograft Assay

Sixteen male BALB/c nude mice (5-week-old) were obtained from Beijing Laboratory Animal Research Center (Beijing, China) and kept in a specific pathogen-free environment. All procedures performed in studies involving animals were approved by author institution. Before tumor transplantation, PANC-1 cells were treated with vehicle (NC), miR-203a-3p mimics or miR-203a-3p inhibitors. PANC-1 cells without treatment were set as Blank group. Each group cells were harvested and injected into the right flank of mice subcutaneously. There were 4 mice in each group. The volume of tumor was recorded every week. The length (L) and width (W) of tumor were measured by calipers, and the volume was calculated according to the formula of $1/2 \times L \times W^2$. Four weeks after injection, mice were sacrificed and tumors were isolated. The expression of miR-203a-3p and SLUG was measured by qRT-PCR. The protein levels of E-cadherin, Twist, N-cadherin, and SLUG were measured by Western blot assay. The GAPDH served as the reference protein.

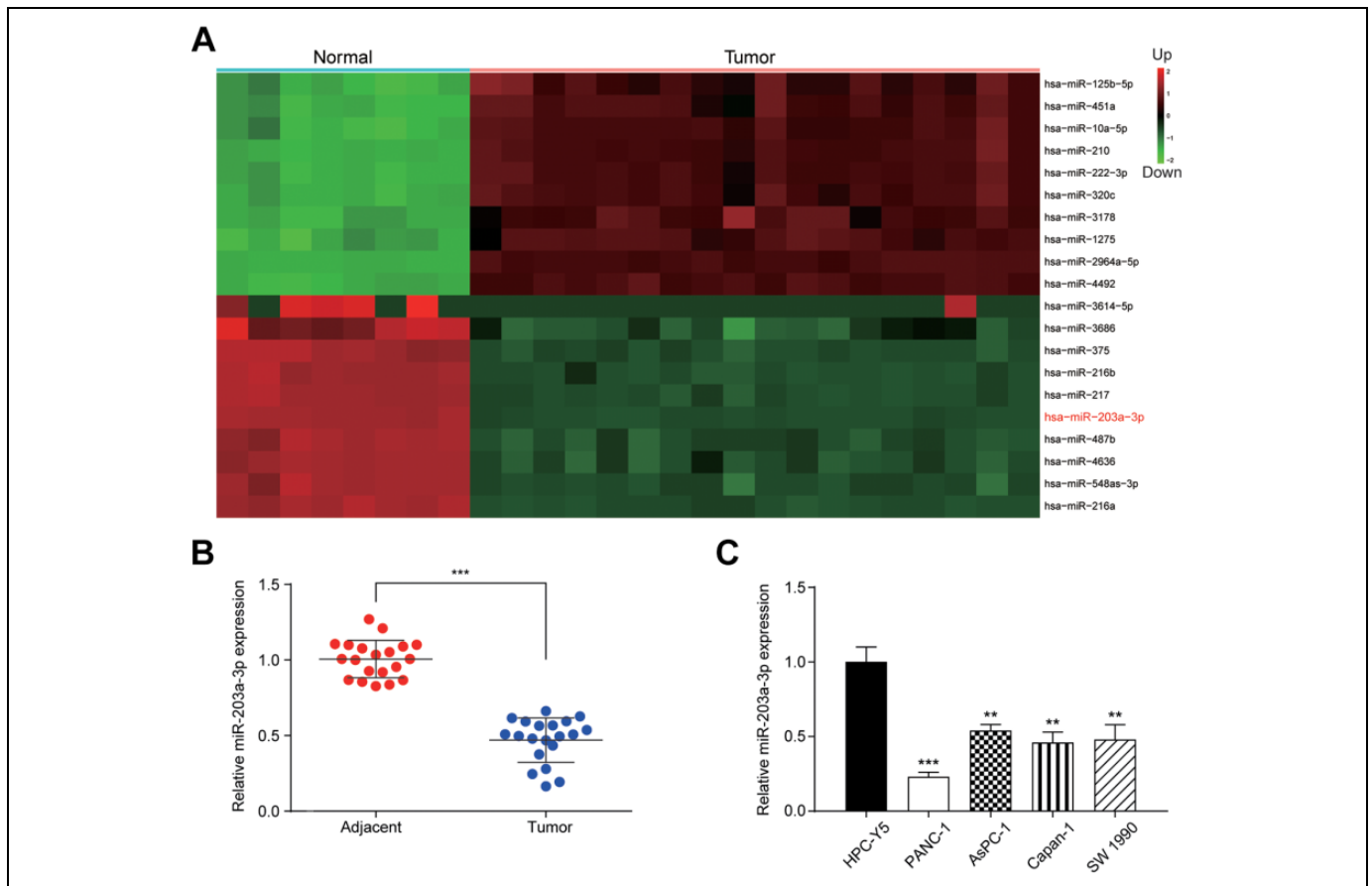


Figure 1. The miR-203a-3p was downregulated in PC. A, Heatmap showed top 10 upregulated and downregulated miRNAs in PC. The red part indicated that genes were upregulated and the green part indicated the downregulation. B, The expression of miR-203a-3p was significantly downregulated in tumor tissues compared to its adjacent normal tissues. C, MiR-203a-3p expression was significantly lower in all 4 PC cell lines compared to pancreatic cell lines. $**P < .01$ and $***P < .001$ compared to the adjacent or HPC-Y5 group. miRNA indicates MicroRNA; PC, pancreatic cancer.

Statistical Analysis

SPSS 21.0 software (IBM, Armonk, New York) and R software were applied to performing statistical analyses. Data were expressed as mean \pm standard deviation.²¹ Two-tailed *t* test was used for comparison between 2 groups. One-way analysis of variance was applied to compare multiple groups. A *P* value $< .05$ is statistically significant.

Results

MiR-203a-3p Expression Was Downregulated in PC Tissues and Cells

To examine the aberrant miRNA expression in PC tissues, we conducted bioinformatics analysis. It was found that a total of 113 miRNA expressed differentially in PC tissues and the top 10 miRNAs with upregulation or downregulation were shown in Figure 1A. As miR-203a-3p has been reported in the previous study⁹ in other cancers except for PC, miR-203a-3p was chosen for our target. miR-203a-3p expression was measured by qRT-PCR. In consistence with the results of the

bioinformatics analysis, the expression of miR-203a-3p in PC tissues was significantly downregulated compared with adjacent normal tissues ($P < .001$; Figure 1B). The expression of miR-203a-3p was notably lower in 4 PC cell lines, including PANC-1, AsPC-1, Capan-1, and SW 1990 cell lines than the normal pancreatic cell line, HPC-Y5 ($P < .01$; Figure 1C). PANC-1 and AsPC-1 cell lines were chosen for further *in vitro* assays.

miR-203a-3p Inhibited PC Cell Proliferation, Migration, Invasion, and EMT Process

To identify the roles of miR-203a-3p on the PC cell proliferation, migration, and invasion, we transfected miR-203a-3p mimics or inhibitors into PANC-1 and AsPC-1 cells. The successful transfection was confirmed as the expression of miR-203-3p was significantly higher in miR-203a-3p mimic-transfected cells and lower in miR-203a-3p inhibitor-transfected cells compared to the NC group ($P < .001$; Figure 2A). Cell Counting Kit-8 assay showed that the proliferation rate of cells decreased dramatically in the miR-203a-3p mimic

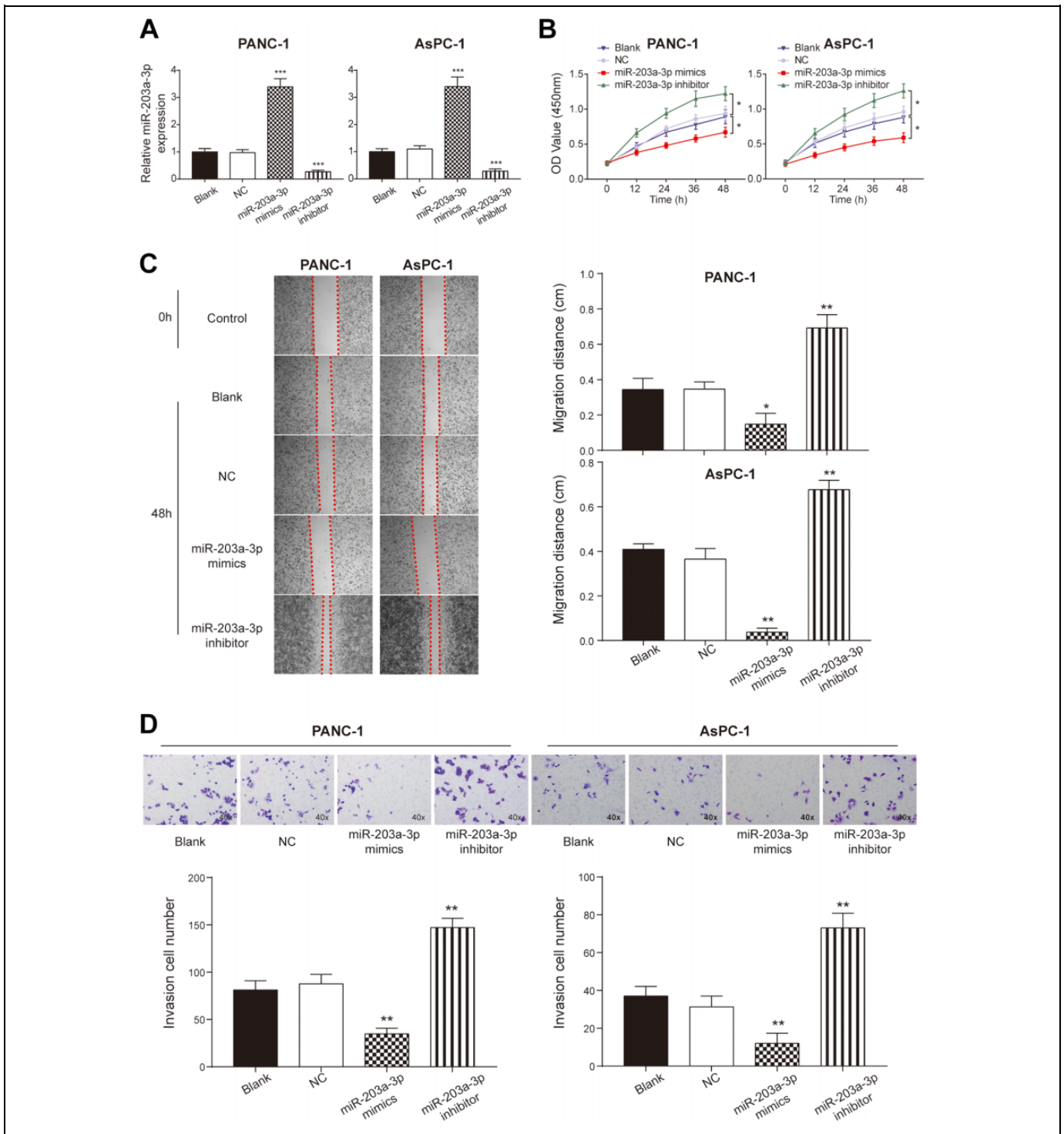


Figure 2. The proliferation, migration, and invasion ability were regulated by miR-203a-3p. A, The expression of miR-203a-3p was significantly upregulated after the transfection of miR-203a-3p mimics and the expression was decreased dramatically after adding the miR-203a-3p inhibitor. B, The Cell Counting Kit-8 assay indicated that the proliferation rate of the PANC-1 and AsPC-1 cells was promoted by transfecting with miR-203a-3p inhibitors and it was inhibited by adding the miR-203a-3p mimics. C, Wound healing assay indicated that the migration ability of PANC-1 and AsPC-1 cells was inhibited by the transfection with miR-203a-3p mimics and was enhanced by the transfection with miR-203a-3p inhibitors. D, Transwell assay illustrated that the invasion ability was promoted by inhibiting the expression of miR-203a-3p compared with the NC group. * $P < .05$, ** $P < .01$, and *** $P < .001$ compared with the NC group. NC indicates negative control.

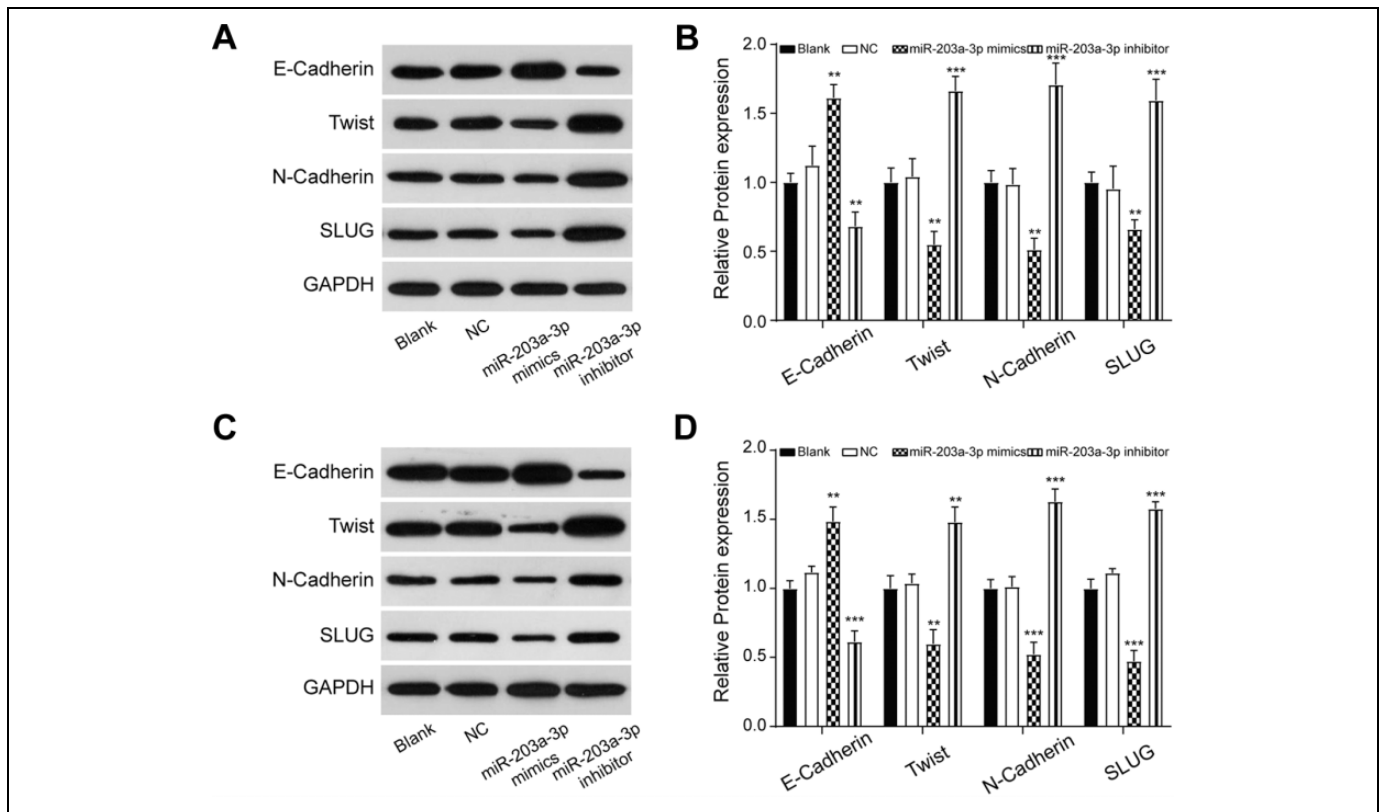


Figure 3. The EMT markers were measured using Western blot assay. The results indicated that higher expression of miR-203a-3p inhibited the process of EMT, while the lower expression of miR-203a-3p plays the reverse role in the PANC-1 (A, B) and AsPC-1 (C, D) cells. $**P < .01$ and $***P < .001$ compared with the NC group. EMT indicates epithelial–mesenchymal transition; NC, negative control.

group in comparison with the NC group ($P < .05$; Figure 2B). Wound-healing assay and transwell assay showed that both the migration distance ($P < .05$; Figure 2C) and the number of invasion cells ($P < .01$; Figure 2D) decreased significantly after transfection with miR-203a-3p mimics, which indicated that the miR-203a-3p suppressed the migration and invasion ability of PC cells. Aiming to confirm the effect of miR-203-3p on EMT, we detected the expression of EMT-related proteins after transfection with miR-203a-3p mimics and inhibitors via Western blot assay. In both cell lines, the expression of E-cadherin was increased, while that of Twist, N-cadherin, and SLUG was decreased following transfection with miR-203a-3p mimics ($P < .01$; Figure 3). In conclusion, miR-203a-3p inhibited PC cell proliferation, migration, invasion, and EMT process.

SLUG Expression Was Upregulated in PC Tissues, Which Was Also a Potential Target of miR-203a-3p

To further investigate how miR-203a-3p regulates EMT process, we conducted further bioinformatics analysis in PC tissues to screen out abnormally expressed mRNAs. Top 10 mRNAs with upregulation or downregulation were shown in Figure 4A. As mentioned in the introduction, SLUG involves the EMT process. Thus, qRT-PCR was used to measure the expression of SLUG in patients' tissues. The expression of

SLUG in PC tissues was significantly higher compared with adjacent healthy tissues ($P < .001$; Figure 4B), which was consistent with the results of bioinformatics analysis. As shown in Figure 4C, miR-203a-3p had the combining site to SLUG. After co-transfection with miR-203a-3p mimics, the luciferase activity of the cells in the SLUG 3'UTR-wt group was significantly decreased in comparison with scramble group ($P < .05$), while no significant difference was found in the co-transfection of miR-203a-3p mimics and SLUG 3'UTR-mut group (Figure 4D). Moreover, RIP results showed that miR-203a-3p and SLUG were enriched in Ago2 immunoprecipitates but not in IgG immunoprecipitates (Figure 4E and F). Therefore, we confirmed that miR-203a-3p directly targeted SLUG.

miR-203a-3p Suppressed the Proliferation, Migration, Invasion, and EMT Process of PC Cells by Targeting SLUG *in vitro*

To further explore whether miR-203a-3p regulates PC cell proliferation, invasion, and migration by targeting SLUG, we performed the *in vitro* assays. The PANC-1 and AsPC-1 cells were transfected with si-SLUG and its transfection efficiency was detected by qRT-PCR that SLUG expression decreased significantly in the si-SLUG group compared to the NC group ($P < .05$; Figure 5A). The cell proliferation, migration distance,

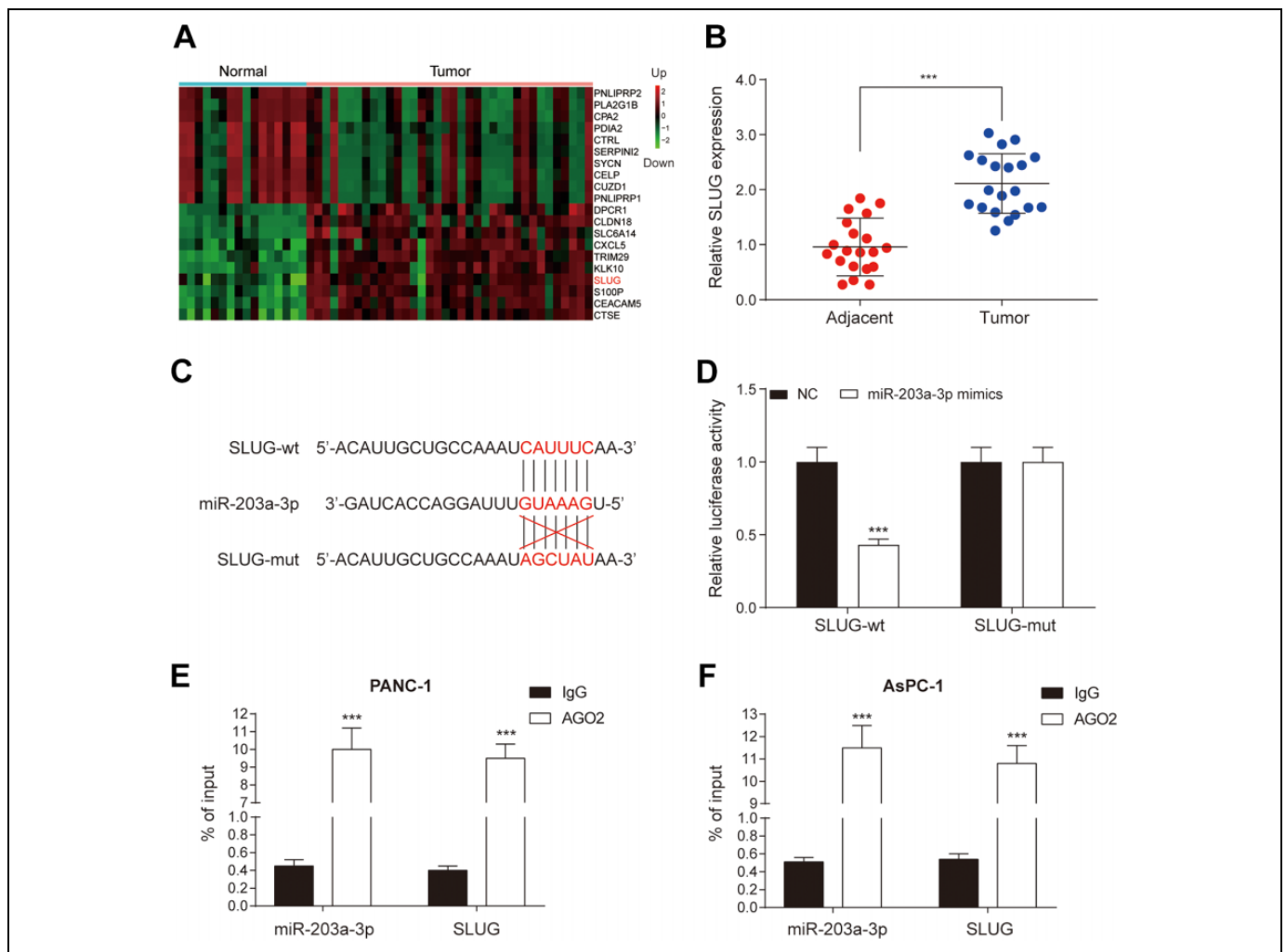


Figure 4. SLUG is one of the targets of miR-203a-3p. A, Heatmap showed top 10 upregulated and downregulated genes in PC. Red part included upregulated genes, while the green part showed downregulated genes. B, Quantitative real-time polymerase chain reaction assay indicated that the expression of SLUG was significantly higher in tumor tissues compared to adjacent normal tissues. C, The combining site of miR-203a-3p and SLUG was revealed. D, The luciferase reporter assay proved that SLUG was a target of miR-203a-3p. E and F, RIP assay showed miR-203a-3p and SLUG were enriched in Ago2 immunoprecipitates but not in IgG immunoprecipitates. *** $P < .001$ compared with adjacent normal tissues, NC group or IgG group. IgG indicates immunoglobulin G; NC, negative control; PC, pancreatic cancer.

and invasion cell number were dramatically decreased after SLUG knockdown ($P < .01$; Figure 5B-D). These decreases were recovered by adding miR-203a-3p inhibitor to cells transfected with si-SLUG. Since SLUG is also one of the important players during EMT process, we measured the expression of EMT-related marker proteins. The Western blot assay showed that the expression of E-cadherin increased, while that of Twist, N-Cadherin, and SLUG decreased in the si-SLUG group compared to the NC group ($P < .01$; Figure 6). By co-transfecting with si-SLUG and miR-203a-3p inhibitors, the expression of these EMT-related proteins were back to normal level in comparison with si-SLUG group ($P < .01$; Figure 6). These results suggested that miR-203a-3p could suppress the proliferation, migration, invasion, and EMT of PC cells via the downregulation of SLUG *in vitro*.

miR-203a-3p Suppressed the PC Progression and EMT Process by Sponging Slug *in vivo*

In vitro assays were verified by the xenograft assay. PANC-1 cells treated with vehicle (NC group), miR-203a-3p mimics, miR-203a-3p inhibitors, or without treatment (Blank group) were injected into nude mice. Tumors from the miR-203a-3p mimic group were significantly smaller than that from the NC group, while that from the miR-203a-3p inhibitor group were significantly larger ($P < .05$; Figure 7A and B). Compared to the NC group, the expression of miR-203a-3p was upregulated in the miR-203a-3p mimic group and downregulated in the miR-203a-3p inhibitor group ($P < .001$; Figure 7C). Moreover, SLUG expression decreased in the miR-203a-3p mimic group and increased in the miR-203a-3p inhibitor group in

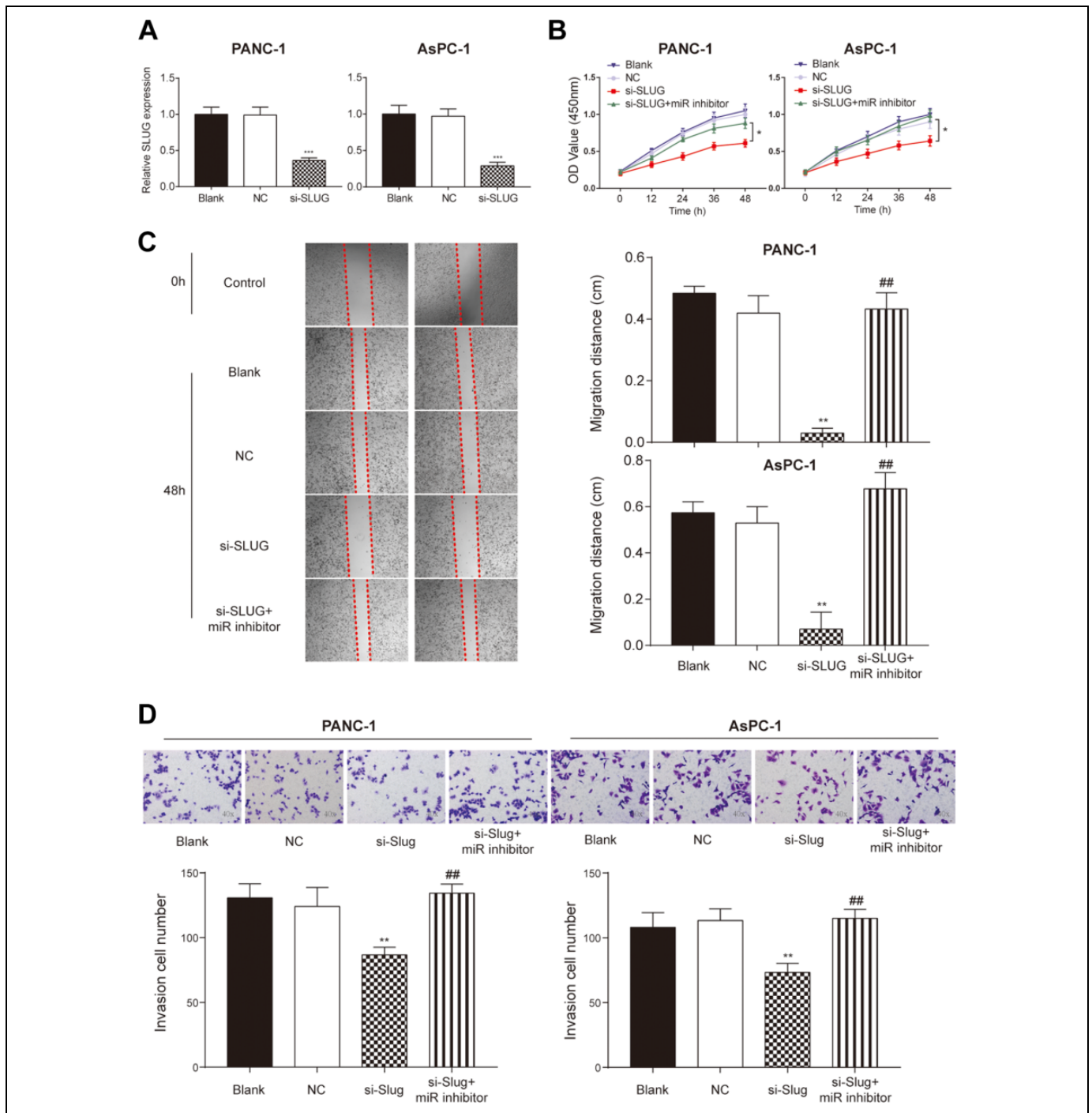


Figure 5. SLUG affected the proliferation, migration, and invasion of PC cells. A, Quantitative real-time–polymerase chain reaction showed that the expression of SLUG was lower after the knockdown of SLUG. B, Cell Counting Kit-8 assay indicated that the proliferation rate was significantly inhibited by the knockdown of SLUG and it was restored in the co-transfected group. C, Wound healing assay indicated that the migration ability of PANC-1 and AsPC-1 cells was inhibited by transfection with si-SLUG and was recovered by adding miR-203a-3p inhibitors. D, Transwell assay illustrated that the invasion ability was inhibited by the knockdown of SLUG and was restored by adding miR-203a-3p inhibitors. * $P < .05$, ** $P < .01$, and *** $P < .001$ compared with NC group; ## $P < .01$ compared with si-SLUG group. NC indicates negative control; PC, pancreatic cancer.

comparison with the NC group ($P < .001$; Figure 7D). The expression of EMT-related proteins was measured by Western blot assay. As shown in Figure 7E and F, E-cadherin level was increased in the miR-203a-3p mimic group, while twist, N-

cadherin, and SLUG levels were decreased ($P < .01$). The situation in the miR-203a-3p inhibitor group was the opposite. These results confirmed that miR-203a-3p inhibited PC development by suppressing the EMT process via sponging SLUG.

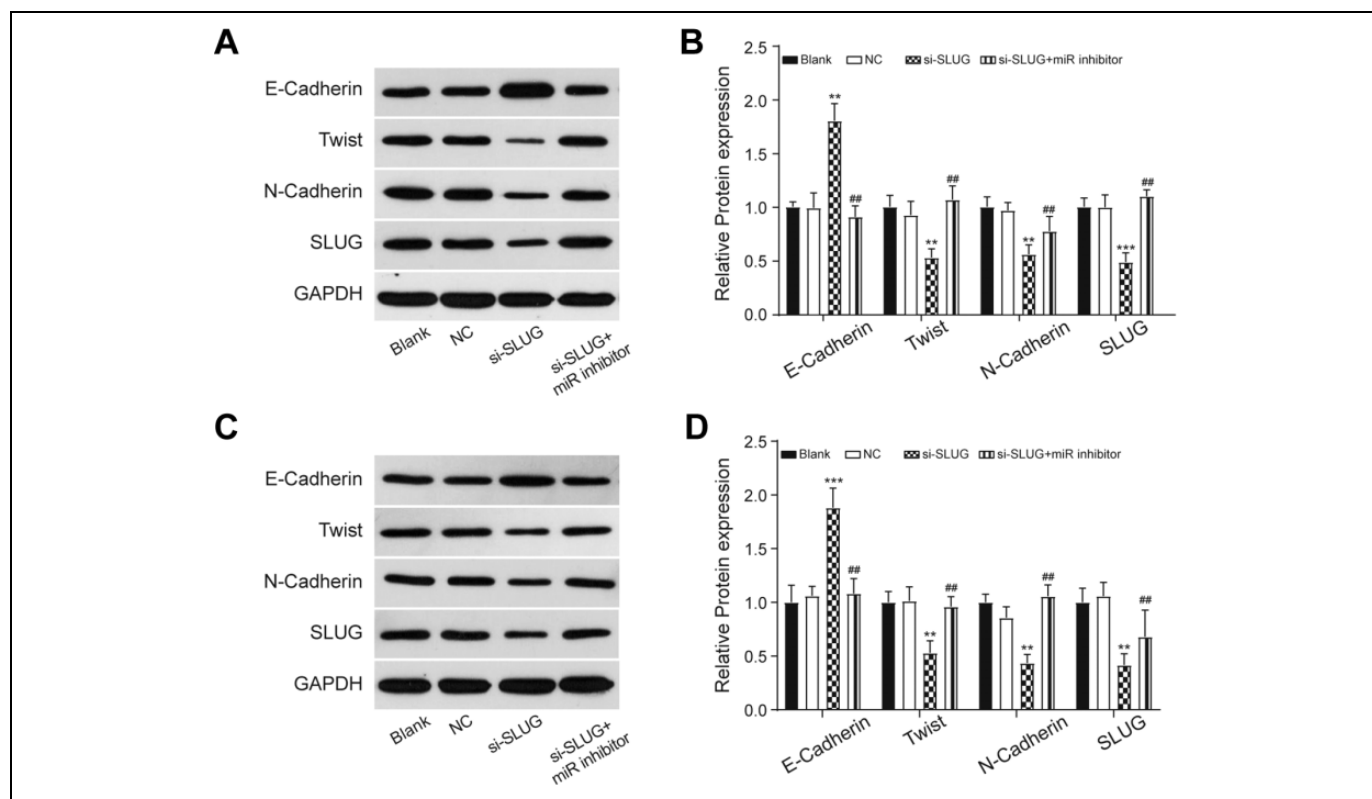


Figure 6. The EMT markers were measured by the Western blot assay. The results indicated that the knockdown of SLUG inhibited the process of EMT in both PANC-1 (A and B) and AsPC-1 (C and D) cell line. ** $P < .01$ and *** $P < .001$ compared with NC group; ### $P < .01$ compared with si-SLUG group. EMT indicates epithelial–mesenchymal transition; NC, negative control.

Discussion

Bioinformatics analysis revealed that miR-203a-3p was down-regulated in the PC tissues. Both *in vitro* and *in vivo* assay illustrated that overexpression of miR-203a-3p inhibited the proliferation, migration, and invasion ability by targeting SLUG and thus suppressed the EMT process.

Under the research by American Cancer Society, the 5-year relative survival rate of PC (8%) is the lowest among cancers and it drops to 3% when patients were diagnosed at a terminal stage.²² The only efficient therapeutics for PC patients is surgery, but no more than 20% of patients are suitable for surgery.²³ Gemcitabine therapy is the first-line treatment for patients who are not eligible for surgical resection, but gemcitabine therapy has limited efficacy for treating metastatic PC.²⁴ The prognosis for PC patients remains depressing, and further efforts towards improved therapeutic options are still urgently required.

Recent works focus on developing the miRNA therapeutics to PC as some of the miRNAs participate in various cellular processes, including cell proliferation, metastasis, apoptosis, and EMT process.^{25,26} Guan *et al* showed that miR-101 inhibited proliferation of breast cancer cells by targeting EYA1.²⁷ In the research by Guo *et al*, they found that the cell invasion and the EMT process of triple negative breast cancer cells were

inhibited by miR-508-3p.²⁸ miR-203a-3p has been widely studied in cancers such as colorectal cancer,²⁹ nasopharyngeal carcinoma,³⁰ and hepatocellular carcinoma,³¹ which indicated that miR-203a-3p plays a key role in the neoplastic process. The current research showed that miR-203a-3p expression was reduced in PC cells and the finding was consistent with the research by Wang *et al* in gastric cancer.⁷

Epithelial–mesenchymal transition process involves in morphogenesis during embryonic development and it also promotes the malignancy in tumor progression.⁷ The molecular mechanisms of EMT are multiple and diverse in human carcinomas.^{32,33} Li *et al* reported that EMT process in colorectal cancer was regulated by the LncRNA H19/miR-194/FoxM1 axis.³³ Wang *et al* revealed that circPTK2 inhibited EMT by regulating transcriptional intermediary factor 1 γ in non-small cell lung cancer.³⁴ In terms of PC, a recent study indicated that the SUMO1P3 might regulate the EMT process³⁵ and Pei *et al* indicated that the EMT process in PC could be inhibited by toosendanin via deactivating the PI3K/AKT and mTOR signaling pathway.³⁶

In the present study, we found that the miR-203a-3p targeting SLUG-mediated EMT process. The upregulation of E-cadherin and the promotion of SNAIL, Twist, and N-cadherin were related to the EMT process.³⁷ Moreover, the zinc finger e-box-binding homeobox 1 (ZEB1) was also a

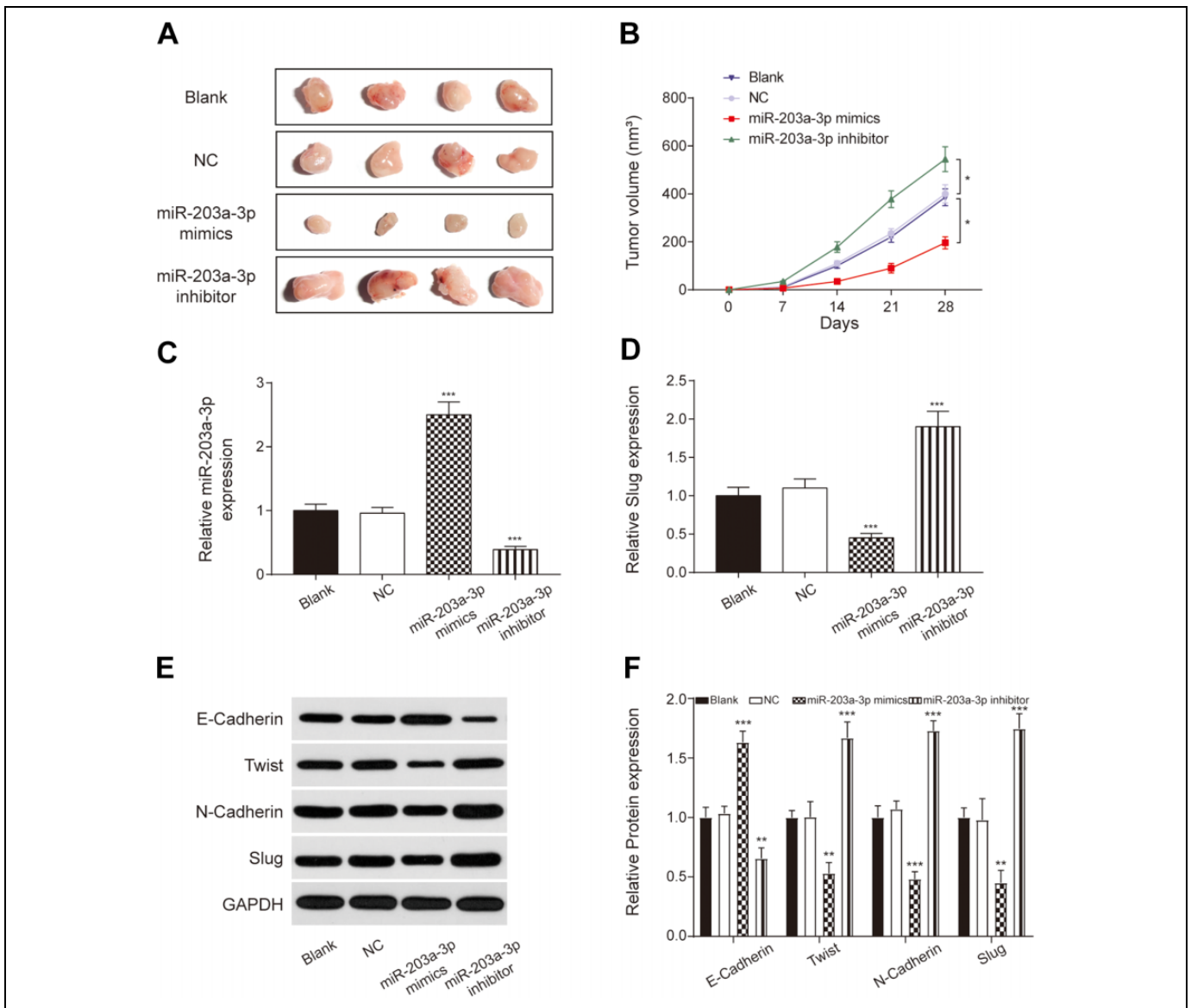


Figure 7. miR-203a-3p inhibited PC progression *in vivo*. A, Tumors isolated from mice at 28 days after injection. B, Changes in tumor volume following injection of PANC-1 cells. C and D, The expression of miR-203a-3p was upregulated, while that of the SLUG was decreased in the miR-203a-3p mimics group. E and F: The epithelial-mesenchymal transition process was inhibited in the miR-203a-3p mimic group, while enhanced in the miR-203a-3p inhibitor group. * $P < .05$, ** $P < .01$ and *** $P < .001$ compared with the NC group. NC indicates negative control; PC, pancreatic cancer.

master regulator of EMT process and ZEB1 deficiency promotes EMT.³⁸ Previous studies have shown that SLUG inhibition dysregulates EMT to represses cancer progression or metastasis,^{39,40} and loss of E-cadherin and amplification of N-cadherin and Twist promotes the EMT process.⁴¹ Consistently, our study showed that after downregulating SLUG, the expression of E-cadherin was increased and that of N-cadherin and Twist were decreased, indicating EMT process was suppressed. Moreover, the current study showed that the alterations caused by downregulating SLUG were restored by adding miR-203a-3p inhibitors. Accordingly, it was concluded that the

downregulation of miR-203a-3p promoted EMT process by enhancing SLUG expression in PC.

Conclusions

In this research, we studied the specific role of miR-203a-3p in PC and noted that the dysregulation of miR-203a-3p might lead to the abnormal expression of SLUG, which advances the EMT process in PC. Our research provides a new perspective for the diagnosis of PC. Since EMT process is closely associated with cancer metastasis, the mechanism of miR-203a-3p inhibiting

the metastasis of PC although EMT is another further research point for us.

Authors' Note

The study design and conception were contributed by N.A. and B.Z. Data analysis and interpretation were done by N.A. and B.Z. Statistical analysis was conducted by N.A. and B.Z. Drafting of the manuscript was done by N.A. and B.Z. Critical revision of the manuscript was done by N.A. and B.Z. All authors have read and approved the final article. All procedures performed in studies involving human participants were in accordance with the ethical standards of the Sichuan Academy of Medical Sciences & Sichuan Provincial People's Hospital. All procedures involving animals were performed in compliance with Shandong Provincial Hospital Affiliated to Shandong University guidelines. Written informed consent was obtained from all individual participants included in the study. The manuscript has not been submitted to more than one journal for simultaneous consideration, and no data have been fabricated or manipulated in this manuscript.

Declaration of Conflicting Interests

The author(s) declared no potential conflicts of interest with respect to the research, authorship, and/or publication of this article.

Funding

The author(s) disclosed receipt of the following financial support for the research, authorship, and/or publication of this article: This work was supported by Scientific Research Projects of Health Commission of Sichuan Province [grant number 16PJ476].

ORCID iD

Bo Zheng  <https://orcid.org/0000-0002-4126-266X>

References

- Akce M, Zaidi MY, Waller EK, El-Rayes BF, Lesinski GB. The potential of CAR T cell therapy in pancreatic cancer. *Front Immunol.* 2018;9:2166. doi:10.3389/fimmu.2018.02166.
- Liu J, Hu G, Gong Y, et al. Silencing of TRPM8 inhibits aggressive tumor phenotypes and enhances gemcitabine sensitivity in pancreatic cancer. *Pancreatol.* 2018;18(8):935-944. doi:10.1016/j.pan.2018.08.011.
- Yang JC, Rosenberg SA. Adoptive T-Cell therapy for cancer. *Adv Immunol.* 2016;130(29):279-294. doi:10.1016/bs.ai.2015.12.006.
- Ahir BK, Lakka SS. Elucidating the microRNA-203 specific biological processes in glioblastoma cells from comprehensive RNA-sequencing transcriptome profiling. *Cell Signal.* 2019;53:22-38. doi:10.1016/j.cellsig.2018.09.014.
- Lewis BP, Burge CB, Bartel DP. Conserved seed pairing, often flanked by adenosines, indicates that thousands of human genes are microRNA targets. *Cell.* 2005;120(1):15-20. doi:10.1016/j.cell.2004.12.035.
- Farazi TA, Hoell JI, Morozov P, Tuschl T. MicroRNAs in human cancer. *Adv Exp Med Biol.* 2013;774:1-20. doi:10.1007/978-94-007-5590-1_1.
- Wang Z, Zhao Z, Yang Y, et al. MiR-99b-5p and miR-203a-3p function as tumor suppressors by targeting IGF-1 R in gastric cancer. *Sci Rep.* 2018;8(1):10119. doi:10.1038/s41598-018-27583-y.
- Zhou Z, Shu B, Xu Y, et al. MicroRNA-203 modulates wound healing and scar formation via suppressing hes1 expression in epidermal stem cells. *Cell Physiol Biochem.* 2018;49(6):2333-2347. doi:10.1159/000493834.
- He J, Deng Y, Yang G, Xie W. MicroRNA-203 down-regulation is associated with unfavorable prognosis in human glioma. *J Surg Oncol.* 2013;108(2):121-125. doi:10.1002/jso.23315.
- Barrallo-Gimeno A, Nieto MA. The Snail genes as inducers of cell movement and survival: implications in development and cancer. *Development.* 2005;132(14):3151-3161. doi:10.1242/dev.01907.
- Peinado H, Olmeda D, Cano A. Snail, zeb and bHLH factors in tumour progression: an alliance against the epithelial phenotype? *Nat Rev Cancer.* 2007;7(6):415-428. doi:10.1038/nrc2131.
- Gupta PB, Kuperwasser C, Brunet JP, et al. The melanocyte differentiation program predisposes to metastasis after neoplastic transformation. *Nat Genet.* 2005;37(10):1047-1054. doi:10.1038/ng1634.
- Phillips S, Kuperwasser C. SLUG: critical regulator of epithelial cell identity in breast development and cancer. *Cell Adh Migr.* 2014;8(6):578-587. doi:10.4161/19336918.2014.972740.
- Liu T, Zhang X, Shang M, et al. Dysregulated expression of Slug, vimentin, and E-cadherin correlates with poor clinical outcome in patients with basal-like breast cancer. *J Surg Oncol.* 2013;107(1):188-194. doi:10.1002/jso.23240.
- Hotz B, Arndt M, Dullat S, Bhargava S, Buhr HJ, Hotz HG. Epithelial to mesenchymal transition: expression of the regulators snail, slug, and twist in pancreatic cancer. *Clin Cancer Res.* 2007;13(16):4769-4776. doi:10.1158/1078-0432.CCR-06-2926.
- Lamouille S, Xu J, Derynck R. Molecular mechanisms of epithelial-mesenchymal transition. *Nat Rev Mol Cell Biol.* 2014;15(3):178-196. doi:10.1038/nrm3758.
- Kalluri R, Weinberg RA. The basics of epithelial-mesenchymal transition. *J Clin Invest.* 2009;119(2):1420-1428. doi:10.1172/JCI39104.
- Zhang Y, Xue X, Zhao X, et al. Vasohibin 2 promotes malignant behaviors of pancreatic cancer cells by inducing epithelial-mesenchymal transition via hedgehog signaling pathway. *Cancer Med.* 2018;7(11):5567-5576. doi:10.1002/cam4.1752.
- Tam WL, Weinberg RA. The epigenetics of epithelial-mesenchymal plasticity in cancer. *Nat Med.* 2013;19(11):1438-1449. doi:10.1038/nm.3336.
- Loyer X, Paradis V, Henique C, et al. Liver microRNA-21 is overexpressed in non-alcoholic steatohepatitis and contributes to the disease in experimental models by inhibiting PPAR alpha expression. *Gut.* 2016;65(11):1882-1894. doi:10.1136/gutjnl-2014-308883.
- Kransdorf MJ. Malignant soft-tissue tumors in a large referral population: distribution of diagnoses by age, sex, and location. *AJR Am J Roentgenol.* 1995;164(1):129-134. doi:10.2214/ajr.164.1.7998525.s.
- Siegel RL, Miller KD, Jemal A. Cancer Statistics, 2017. *CA Cancer J Clin.* 2017;67(1):7-30. doi:10.3322/caac.21387.

23. Rahib L, Smith BD, Aizenberg R, Rosenzweig AB, Fleshman JM, Matrisian LM. Projecting cancer incidence and deaths to 2030: the unexpected burden of thyroid, liver, and pancreas cancers in the United States. *Cancer Res.* 2014;74(11):2913-2921. doi:10.1158/0008-5472.CAN-14-0155.
24. Von Hoff DD, Ervin T, Arena FP, et al. Increased survival in pancreatic cancer with nab-paclitaxel plus gemcitabine. *N Engl J Med.* 2013;369(18):1691-1703. doi:10.1056/NEJMoa1304369.
25. Ferino A, Miglietta G, Picco R, Vogel S, Wengel J, Xodo LE. MicroRNA therapeutics: design of single-stranded miR-216b mimics to target KRAS in pancreatic cancer cells. *RNA Biol.* 2018;15(10):1273-1285. doi:10.1080/15476286.2018.1526536.
26. Zhu G, Zhou L, Liu H, Shan Y, Zhang X. MicroRNA-224 promotes pancreatic cancer cell proliferation and migration by targeting the TXNIP-Mediated HIF1alpha pathway. *Cell Physiol Biochem.* 2018;48(4):1735-1746. doi:10.1159/000492309.
27. Guan H, Dai Z, Ma Y, Wang Z, Liu X, Wang X. MicroRNA-101 inhibits cell proliferation and induces apoptosis by targeting EYA1 in breast cancer. *Int J Mol Med.* 2016;37(6):1643-1651. doi:10.3892/ijmm.2016.2557.
28. Guo SJ, Zeng HX, Huang P, Wang S, Xie CH, Li SJ. MiR-508-3p inhibits cell invasion and epithelial-mesenchymal transition by targeting ZEB1 in triple-negative breast cancer. *Eur Rev Med Pharmacol Sci.* 2018;22(19):6379-6385. doi:10.26355/eurrev_201810_16050.
29. Xiao Z, Qu Z, Chen Z, et al. LncRNA HOTAIR is a prognostic biomarker for the proliferation and chemoresistance of colorectal cancer via MiR-203a-3p-mediated Wnt/ss-catenin signaling pathway. *Cell Physiol Biochem.* 2018;46(3):1275-1285. doi:10.1159/000489110.
30. Jiang N, Jiang X, Chen Z, et al. MiR-203a-3p suppresses cell proliferation and metastasis through inhibiting LASP1 in nasopharyngeal carcinoma. *J Exp Clin Cancer Res.* 2017;36(1):138. doi:10.1186/s13046-017-0604-3.
31. Huo W, Du M, Pan X, Zhu X, Gao Y, Li Z. MiR-203a-3p.1 targets IL-24 to modulate hepatocellular carcinoma cell growth and metastasis. *FEBS Open Bio.* 2017;7(8):1085-1091. doi:10.1002/2211-5463.12248.
32. Han Y, Guo W, Ren T, et al. Tumor-associated macrophages promote lung metastasis and induce epithelial-mesenchymal transition in osteosarcoma by activating the COX-2/STAT3 axis. *Cancer Lett.* 2019;440-441:116-125. doi:10.1016/j.canlet.2018.10.011.
33. Li CF, Li YC, Wang Y, et al. The effect of LncRNA H19/miR-194-5p axis on the epithelial-mesenchymal transition of colorectal adenocarcinoma. *Cell Physiol Biochem.* 2018;50(1):196-213. doi:10.1159/000493968.
34. Wang L, Tong X, Zhou Z, et al. Circular RNA hsa_circ_0008305 (circPTK2) inhibits TGF-beta-induced epithelial-mesenchymal transition and metastasis by controlling TIF1gamma in non-small cell lung cancer. *Mol Cancer.* 2018;17(1):140. doi:10.1186/s12943-018-0889-7.
35. Tian C, Jin Y, Shi S. Long non-coding RNA SUMO1P3 may promote cell proliferation, migration, and invasion of pancreatic cancer via EMT signaling pathway. *Oncol Lett.* 2018;16(2):6109-6115. doi:10.3892/ol.2018.9378.
36. Pei Z, Fu W, Wang G. A natural product toosendanin inhibits epithelial-mesenchymal transition and tumor growth in pancreatic cancer via deactivating Akt/mTOR signaling. *Biochem Biophys Res Commun.* 2017;493(1):455-460. doi:10.1016/j.bbrc.2017.08.170.
37. Serrano-Gomez SJ, Maziveyi M, Alahari SK. Regulation of epithelial-mesenchymal transition through epigenetic and post-translational modifications. *Mol Cancer.* 2016;15:18. doi:10.1186/s12943-016-0502-x.
38. Frausto RF, Chung DD, Boere PM, et al. ZEB1 insufficiency causes corneal endothelial cell state transition and altered cellular processing. *PLoS One.* 2019;14(6):e0218279. doi:10.1371/journal.pone.0218279.
39. Chien MH, Lin YW, Wen YC, et al. Targeting the SPOCK1-snail/sluc axis-mediated epithelial-to-mesenchymal transition by apigenin contributes to repression of prostate cancer metastasis. *J Exp Clin Cancer Res.* 2019;38(1):246. doi:10.1186/s13046-019-1247-3.
40. Lin S, Zhang C, Liu F, et al. Actinomycin V inhibits migration and invasion via suppressing snail/sluc-mediated epithelial-mesenchymal transition progression in human breast cancer MDA-MB-231 cells in vitro. *Mar Drugs.* 2019; 17(5):E305. doi:10.3390/md17050305.
41. Chen H, Pan J, Zhang L, et al. Downregulation of estrogen-related receptor alpha inhibits human cutaneous squamous cell carcinoma cell proliferation and migration by regulating EMT via fibronectin and STAT3 signaling pathways. *Eur J Pharmacol.* 2018;825(2):133-142. doi:10.1016/j.ejphar.2018.02.025.